Horizon 2020 MSCA-ITN-2017

(Marie Skłodowska-Curie Innovative Training Networks)

Project Number: 764461

Acronym: VisIoN

Project title: Visible light based Interoperability and Networking

Work Package WP3: Smart Transportation

Deliverable D3.1: Channel models for Vehicular Visible Light Communications

Prof. Dr. Murat Uysal (WP3 Lead)

April 30, 2019

1. WP objectives

Intelligent Transportation Systems (ITSs) build upon cooperation, connectivity, and automation of vehicles and are expected to improve the safety, efficiency, and sustainability of passenger and freight transportation while enhancing the comfort of driving. Vehicle-to vehicle (V2V), vehicle-to-infrastructure (V2I) and infrastructure-to-vehicle (I2V) communications, commonly referred to as V2X, are key connectivity components for the practical implementation of ITSs. Existing research activities and standardization efforts on V2X have mainly focused on radio frequency (RF) technologies. The impact of current V2X communications on the RF spectrum usages is negligible due to low levels of current market penetration. However, with the widespread adoption of ITSs in the near future, limited RF bands licensed for ITSs can quickly suffer from high interference levels particularly in high-density traffic scenarios. Channel congestion will result in longer delays and degrade the packet rate. To address such shortcomings of RF-based solutions, visible light communication (VLC) has been proposed as an alternative or complementary technology to RF-based V2X communications.

Vehicular VLC is in its infancy in many aspects and requires further research efforts in several areas which this WP aims to address. For example, most works on the propagation modelling and characterization of VLC channels are mainly limited to the indoor environment. For the vehicular networking, special attention should be devoted to mobility as well as to the atmospheric channel. A new key concept to enable connectivity in vehicular VLC is that of multi-hop transmission, where the signal transmitted from the source vehicle can reach the destination vehicle through a number of intermediate vehicles termed "relays." There are also other design considerations in the upper layers that require special attention to realize a fully functional vehicular VLC network. For example, medium access (MAC) protocols for RF systems have been investigated in the literature assuming isotropic radiation of sources. VLC systems with their inherent directionality render conventional MAC schemes practically useless. Hybrid VLC/RF links will also be investigated to ensure link availability at all weather conditions.

In light of the above open research topics, the **overall objective** of this WP is to develop VLC-based wireless access solutions for V2V and V2I/I2V communications. Towards this overall objective, four tasks (each assigned primarily to an ESR) were defined with the **following objectives**:

Task 3.1 Channel modelling and characterization (ESR 8): The objective is to develop realistic outdoor VLC channel models applicable for V2V and V2I/I2V scenarios and characterize the performance of vehicular VLC systems in different weather and environmental conditions.

Task 3.2. Physical (PHY) layer design (ESR 9): The objective is to develop a robust PHY layer design based on multi-hop transmission techniques to enable connectivity between distant vehicles and analyse their performance in various deployment scenarios.

Task 3.3. Networking design (ESR 10): The objective is to develop efficient MAC and upper-layer communication protocols for vehicular VLC links.

Task 3.4. Proof-of-concept implementation (ESR 11): The objective is to develop a custom-design testbed and experimentally verify the feasibility of vehicular VLC links.

2. WP general progress

As will be detailed in this deliverable, ESR 8 (responsible for Task 3.1) used non-sequential ray tracing approach and obtained channel impulse responses (CIRs) for various vehicular scenarios in different weather conditions. Based on these CIRs, he developed closed-form path loss expressions and quantified the effect of various weather conditions such as fog and rain on the vehicular system performance. He further determined the achievable transmission distances through a single hop.

ESR 9 (responsible for Task 3.2) developed a comprehensive mathematical system model which is the basis for the performance evaluation and simulation of PHY layer of vehicular VLC systems. She is currently working on a link budget analysis for vehicular VLC links to determine the required transmit power and other system specifications.

ESR 10 (responsible for Task 3.3) investigated “network bonding” as an enabler for hybrid VLC/RF system design which can be used for purposes of either high availability, load-balancing, maximum throughput or a combination of these. She is currently working on the development of an NS3 network simulator which will be the basis for the evaluation of MAC layer protocols for VLC.

ESR 11 (responsible for Task 3.4) developed an experimental testbed using popular software defined evaluation platform (known as USRPs) and custom-design VLC front-end. He implemented orthogonal frequency division multiplexing (OFDM)-based PHY layer on this testbed and experimentally demonstrated the bit error rate of OFDM VLC systems. He is currently working on the modifications of a donated vehicle for outdoor tests.

3. Progress on "Channel modelling and Characterization"

3.1 Channel Modeling Approach

Our study is based on Zemax®; a commercial optical and illumination design software [1]. We take advantage of the advanced ray tracing features of this software which allows an accurate description of the interaction of rays emitted from the lighting source within a specified confined space.

The major steps of channel modelling approach are provided in Fig. 1. First, a 3D model of vehicular scenario (including vehicles, road, traffic lights etc) is constructed in Zemax®. As inputs, we provide the specifications of vehicular light sources acting as transmitters (i.e., spectral power distribution and intensity distribution) and photodetectors placed on the vehicles for reception (i.e., location on the vehicle, aperture size and field of view).

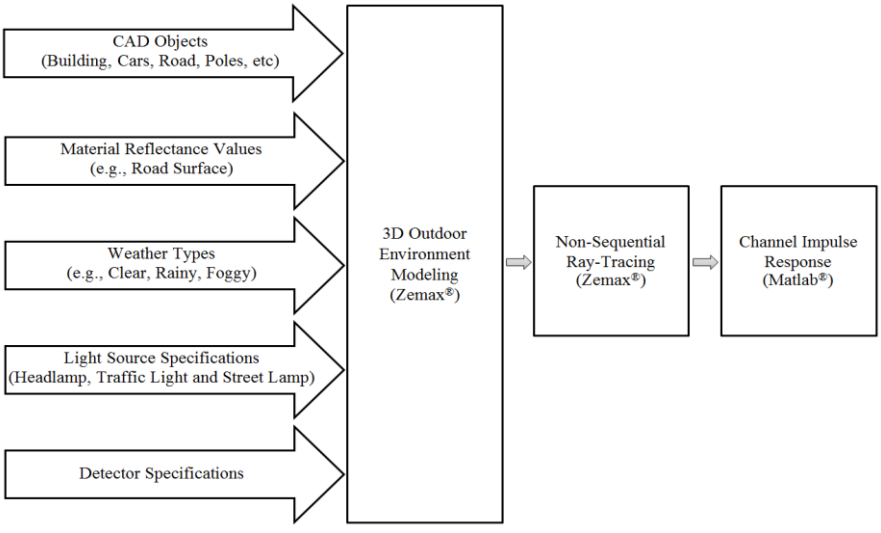

Fig. 1 Steps of channel modeling approach

In simulation environment, we further specify the optical characteristics of the vehicle coating and road surface by defining their wavelength-dependent reflectance values. The road-surface classifications are given in Table 1 [2]. To reflect the effects of weather conditions, we need to define the atmospheric propagation medium. "Bulk Scatter" function in the software allows providing the refractive index, radius and density of particles as input parameters based on Mie model [3, Chapter 3]. The associated values for various weather types are given in Table 2 [4].

Table 1. Road surface classifications [2]

Class	Road Surface Composition	Mode of Reflectance
R1	Asphalt with aggregate including a minimum of 15% artificial brightener aggregate	Mostly diffuse
R2	Asphalt with aggregate including a minimum of 60% gravel sized larger than 10 mm Asphalt with aggregate including a minimum of 10-15% artificial brightener aggregate	Mixed diffuse and specular
R3	Asphalt with dark aggregate-the surface becomes rough after several months of use	Slightly specular
R4	Very smooth asphalt	Mostly specular

Table. 2. Characteristic of various weather types [4]

	Particle Index	Size (μm)	Density (cm^{-3})
Clear Weather	1.000277	10^{-4}	10^{19}
Rain	1.33	100	0.1
Moderate Fog, Visibility = 500 m	1.33	10	12.45
Thick Fog, Visibility = 250 m	1.33	10	24.91
Dense Fog, Visibility = 50 m	1.33	10	124.6

After we create the simulation environment, we use non-sequential ray tracing to determine the channel impulse response (CIR). Zemax® generates an output file including the received power and path length from source to detector for each ray. This is then imported into the numerical computation software MATLAB® to generate the multipath CIR. Let N_P denote the number of PDs. For a given transmission distance, let P_{ij} and τ_{ij} respectively denote the power and the propagation delay of the i^{th} ray received by the j^{th} PD, $j = 1,...N_P$. The CIR at the j^{th} PD can be therefore written as

$$h_j(t) = \sum_{i=1}^{N_j} P_{ij}\delta(t - \tau_{ij}) \quad (1)$$

where δ is the Dirac delta function and N_j is the number of rays received by the j^{th} PD. In simulations, the total optical power of transmitters is assumed to be unity. The CIR can be then scaled for the given value of transmit power P_t. The received power can be therefore calculated as

$$P_r = P_t \sum_{j=1}^{N_p} \int_0^{\infty} h_j(t)dt \ . \quad (2)$$

3.2 Vehicular Scenarios

In our study, we consider four typical vehicular scenarios as detailed below.

Scenario I: V2V communications in the same road lane. As illustrated in Fig.2, we assume that two cars are located at the center of the same lane with a width of *L* and separated with an inter-vehicle distance of d.

Scenario II: V2V communications while changing lanes. As illustrated in Fig.3, we assume that two cars are initially located in different lanes. The driver of the trailing car car starts to change his/her current lane varying the horizontal separation distance between the two cars (indicated by d_h in the figure).

Scenario III: I2V communications. As illustrated in Fig.4, we consider the communication from traffic light (infrastructure) to the car. The traffic light has a height of h. The distance between the car and the traffic light is d and horizontal separation (measured from the center of the car*)* is d_h.

Scenario IV: V2I communications. This is identical to Scenario III where the direction of communication is now from the car to traffic light (infrastructure).

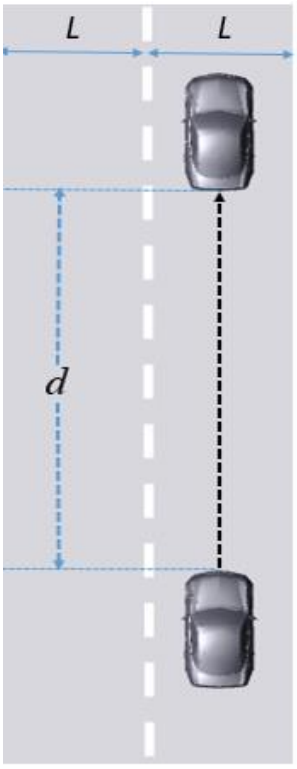

Fig. 2 Scenario I: V2V communications in the same road lane

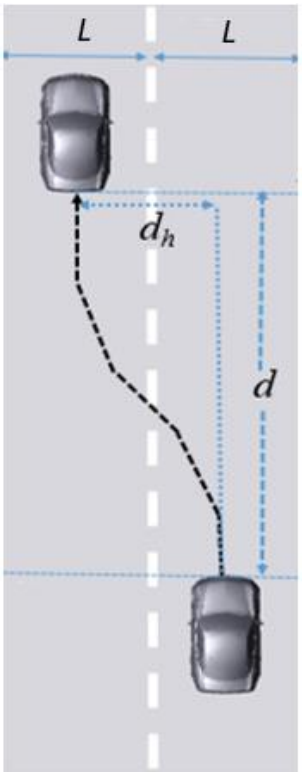

Fig. 3 Scenario II: V2V communications while changing lanes

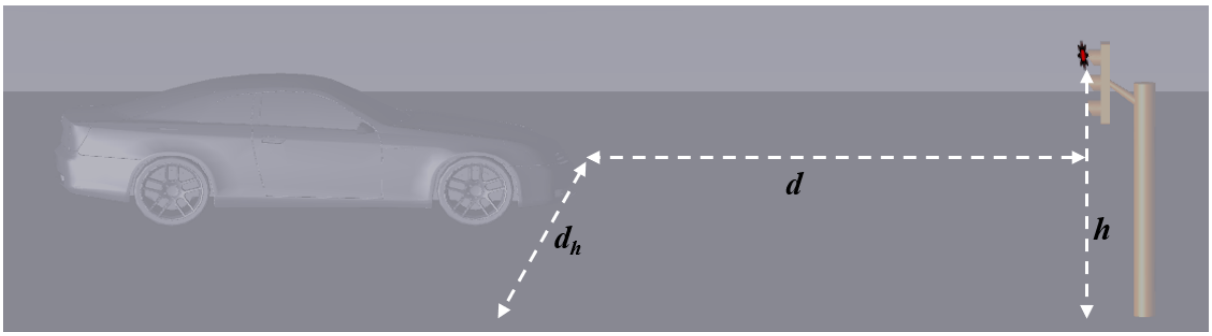

Fig. 4. Scenarios III and IV: I2V/V2I communications

3.3. Simulation Study and Proposed Channel Models

In our simulation study, we assume that cars are black-coloured and modeled as CAD objects with dimensions of 4.6 m × 1.8 m × 1.3 m following Audi A5 Coupe specifications [5]. As illustrated in Fig.5, the headlamps of the vehicles serve as wireless transmitters denoted by TX1 and TX2. We consider the use of Philips Luxeon Rebel white LED for this purpose. The relative spectral power distribution and intensity pattern of headlamps are shown in Fig. 6. We assume that the car is equipped with 5 photodetectors (PDs) as shown in Fig. 7. PD1, P2 and PD3 are located at the back of the car while PD4 and PD5 are installed on the top of side mirrors. It should be noted that all PDs are not necessarily used simultaneously. In the following, when we discuss the simulation results, we specify which PDs were used in each simulation scenario.

Fig. 5 Location of transmitters on the car

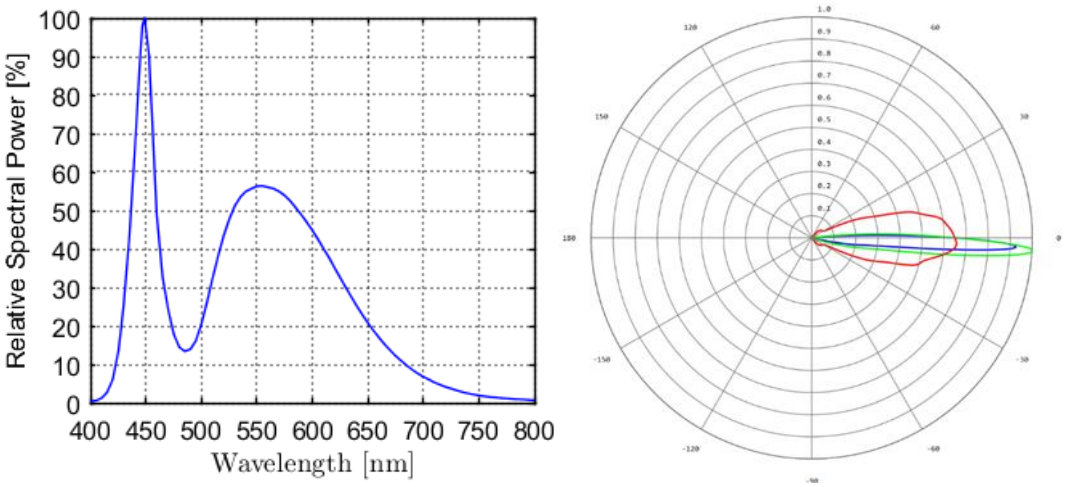

(a) (b)

Fig. 6 (a) Relative spectral power distribution **(b)** Intensity pattern of headlamps with different cross sections

Fig. 7 Location of the photodetectors on the car

As illustrated in Fig.8, the traffic light (red signal) serves as the transmitter in Scenario III. In Scenario IV, photodetectors located on the traffic light (PD A, PD B, PD C) serve as the receivers. The relative spectral power distribution and intensity pattern of red traffic light are shown in Fig. 9.

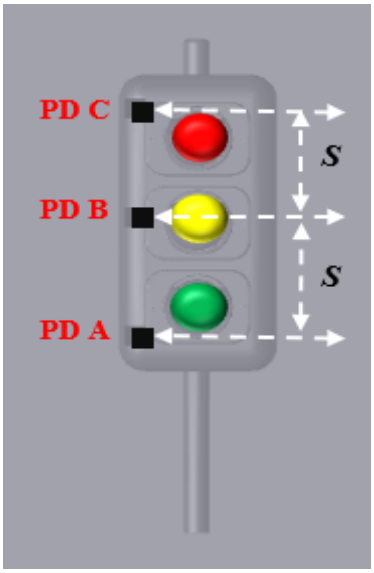

Fig. 8. Location of photodetectors on the traffic light

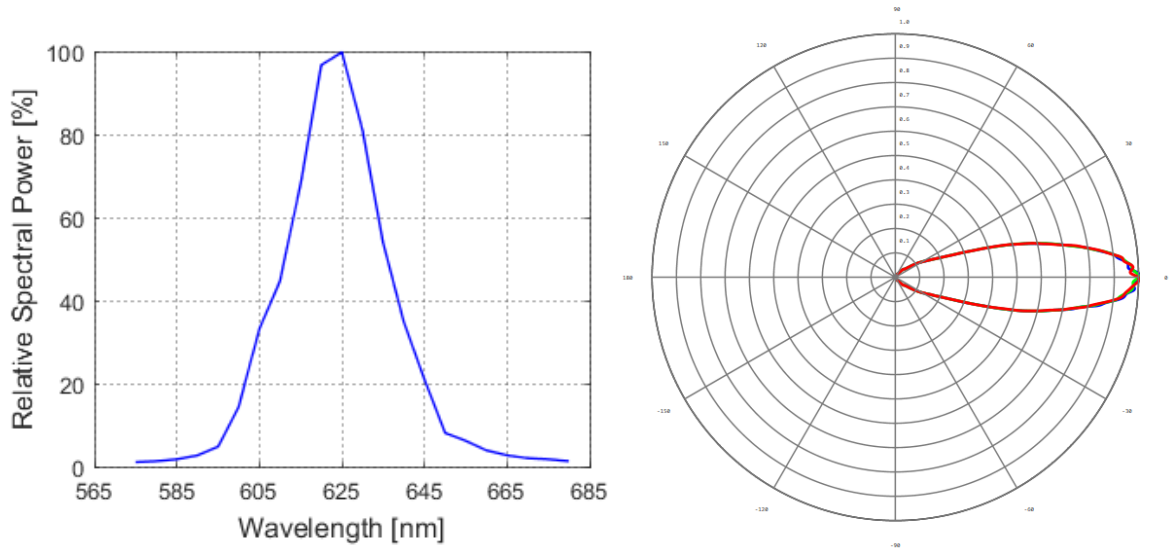

(a) (b)

Fig. 9 (a) Relative spectral power distribution **(b)** Intensity pattern of red traffic light with different cross sections

In our simulation study, we first consider Scenario I where two cars in the same road lane communicate with each other. We consider a lane width of L =3.75 m, typical for the majority of EU countries [6]. We assume road type R2. As specified in Table 1, this corresponds to asphalt with aggregate including a minimum of 60% gravel sized larger than 10 mm or asphalt with aggregate including a minimum of 10-15% artificial brightener aggregate. Using specifications for different weather types provided in Table 2, we obtain the CIRs for clear weather, rain, moderate fog, thick fog, and dense fog for a range of 50 meters with 1 meter increments, i.e., *d*=1,2…. 50 m. In Figs. 10 and 11, we provide some sample CIRs for distances of 10 m and 30 m assuming an aperture size of D_R = 1 cm and field of view of ϕ = 180˚. In this simulation, we assume that only PD 1 (see Fig.7) is employed.

Based on the CIRs obtained for the range of 50 meters, we developed a path loss expression which is applicable for different weather types. The received optical power at a distance d can be written as

$$P_r = P_t G_e G_{att} \tag{3}$$

where G_{at} represents the atmospheric attenuation and changes according to weather conditions. According to Beer-Lambert formula [3], it can be expressed as $G_{att} = \exp\ -cd$ where *c* is the extinction coefficient. G_e is the geometrical loss due to spreading of the emitted optical beam along the distance between the transmitter and the receiver. To take into account the asymmetrical pattern of high-beam source, we use

$$G_e = Ad^{-2B} \tag{4}$$

where A represents the geometrical loss value at a reference distance specified as d_0 and *B* is the decaying factor. Replacing G_{at} and G_e in (2), we can express the path loss model as

$$P_r = P_t \underbrace{Ad^{-2B} \exp\ -cd}_{\rho} \tag{5}$$

where ρ is the optical channel coefficient. In order to determine A and B, we determine the received optical power at a reference distance $d_0 = 10$ m via Zemax® simulations. Let P_0 denote the received optical power at $d_0 = 10$ m. We can then determine *A* as $A = P_0 {d_0}^{2B} \exp\ cd_0\ / P_t$. Through our simulation results, the value of *B* is determined to be 0.87 for clear and rainy weathers while in case of foggy weather, it is determined to be 0.7. The received power versus distance is provided in Fig. 11. It is observed that the proposed expression in (5) provides an excellent match to simulation results. Using these models, we further determined the achievable transmission distance. Those results can be found in our relevant publications (see Section 4).

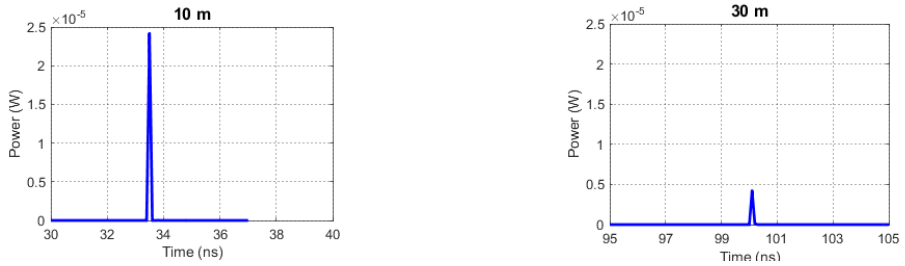

(a)

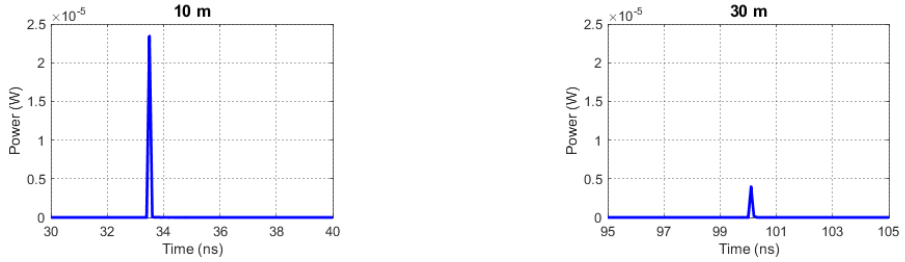

(b)

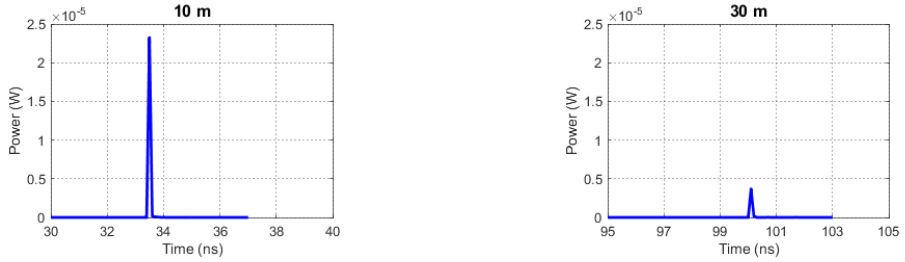

(c)

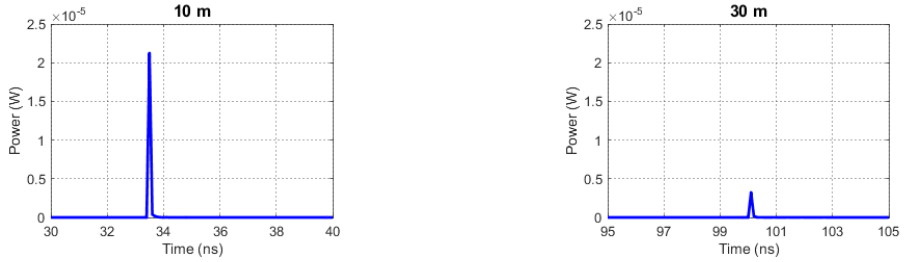

(d)

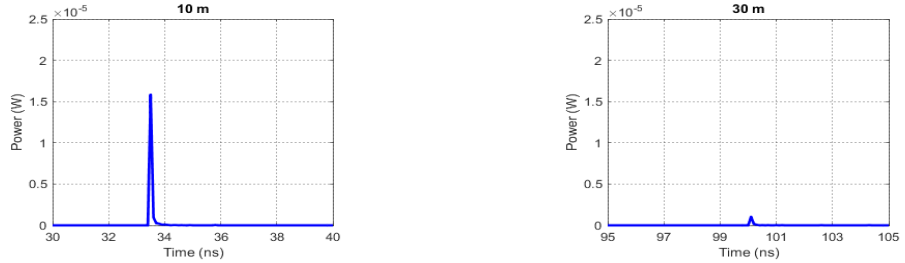

(e)

Fig. 10 Sample CIRs for *d*=10 m and 30 m assuming (a) Clear (b) Rain (c) Moderate fog, (d) Thick fog, and (e) Dense fog.

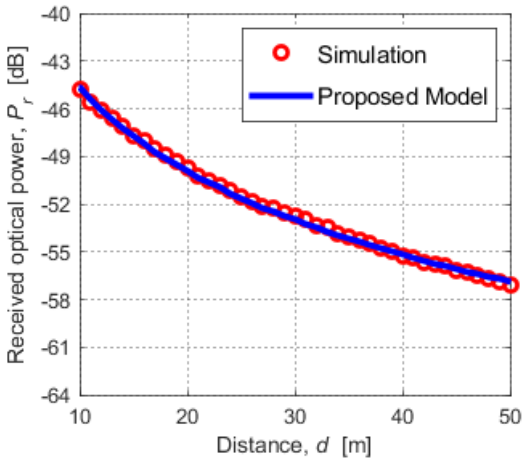

(a)

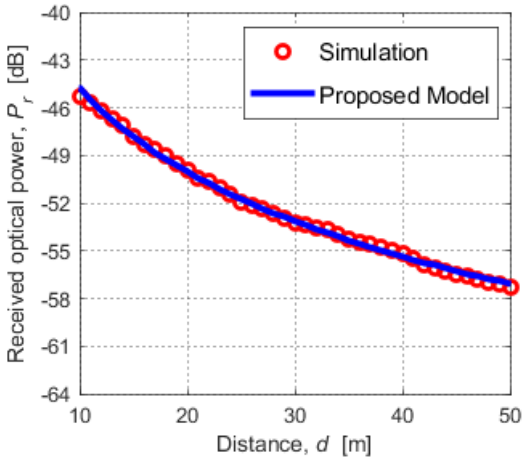

(b)

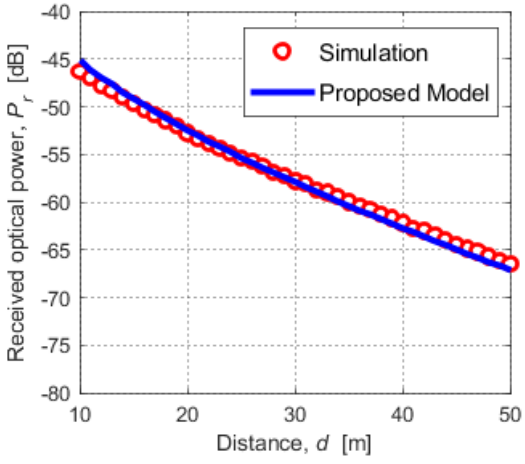

(c)

Fig. 11. Comparison of proposed path loss expression and simulation results for (a) clear weather (b) rainy weather (c) dense fog

In Fig. 12, we consider the use of two photodetectors (PD 2 and PD 3) and quantify the improvement over the single photodetector case earlier considered in Fig. 11. Each of these photodetectors has an aperture size of D_R = 1 cm and field of view of ϕ = 180˚.

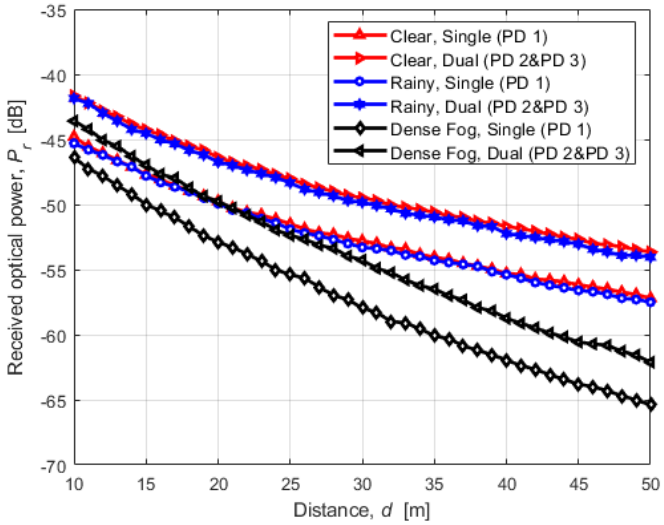

Fig. 12 Performance improvements due to dual photodetector deployment in Scenario I.

In Fig.13, we consider Scenario II (see Fig.3) which deals with V2V communications while changing lanes. We consider the use of four photodetectors (PD 2, PD 3, PD 4, and PD 5) each with aperture size of D_R = 1 cm and field of view of ϕ = 180˚. The PD with maximum received power is selected. Due to deployment of multiple PDs, connectivity is successfully maintained even with imperfect alignments between transmitters and receivers.

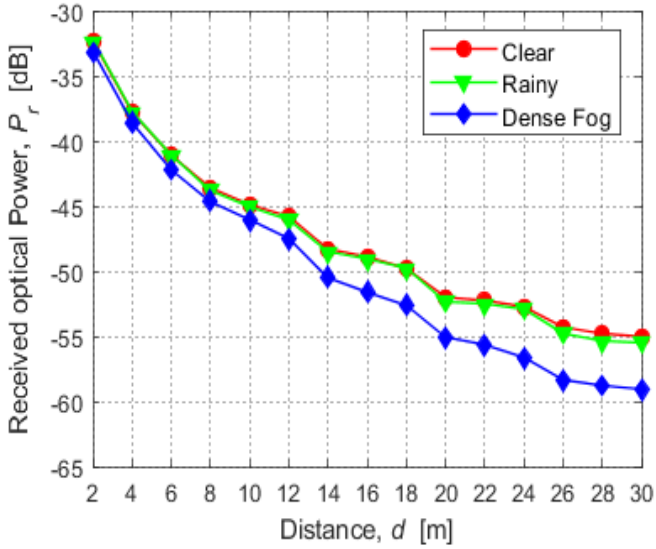

Fig. 13 Received optical power versus distance in Scenario II.

In Fig. 14, we consider Scenario III which deals with I2V communications from the traffic light to the car. We assume the use of either PD 4 or PD 5. Each of them has an aperture size of D_R = 1 cm and field of view of ϕ = 180˚. The height of traffic light is h =2 m [7]. The horizontal separation between the car and the traffic light is d_h = 1 m. We provide some sample CIRs at distances of 25 m and 50 m. It is observed that when the car moves at the right road lane, the received power using the right photodetector (PD 4) is higher than that is received by the left one (PD 5). It can be readily verified that when the car moves at the left lane, PD 5 will be more favourable.

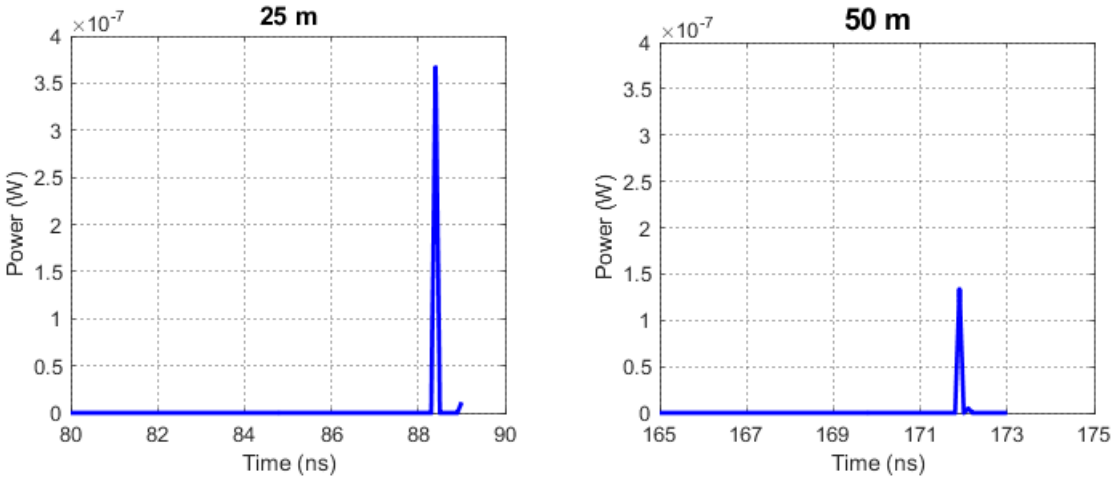

(a)

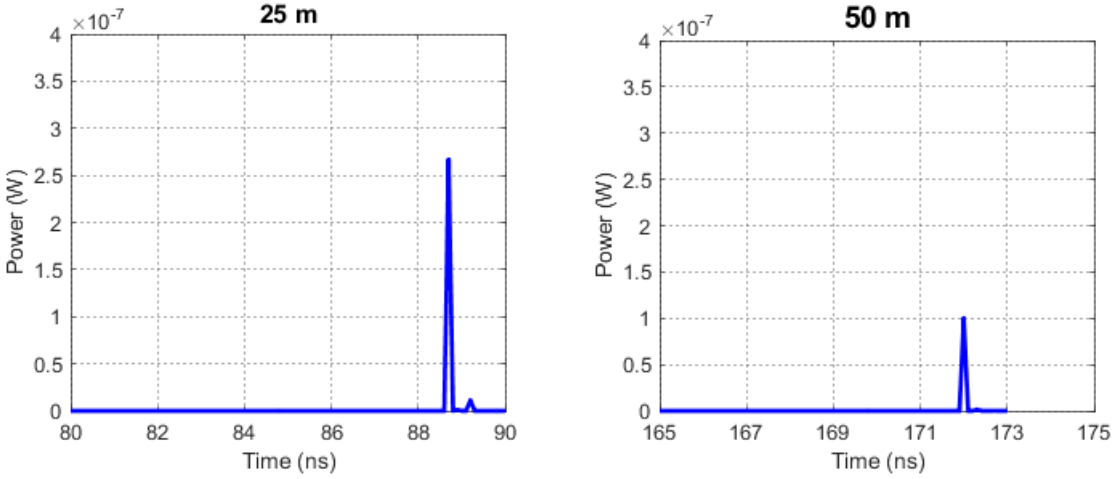

(b)

Fig. 14 Sample CIRs for Scenario III using: (a) PD 4 (b) PD 5

In Fig.15, we consider Scenario IV which deals with V2I communications from the car to traffic light (infrastructure). As illustrated in Fig. 8, the traffic light has three photodetectors (PD A, PD B, and PD C). Each of these has an aperture size of 1 cm and field of view of 180^{o}. The vertical separation *S* between the PDs is assumed to be 0.25 m. It can be observed from our simulation results that the CIRs have more than one peak if the distance between the car and traffic light is short (see CIRs for *d*=20m). This is due to the fact that signals with different travelling distances will have different arrival times. For longer communication distance, the separation difference between the two headlamps are ignorable compared to such distances. Consequently, they act as one source and the resulting CIRs tend to one peak as shown for *d* = 50 m. It is also observed that the PD A has the highest received power due to its relatively lower height.

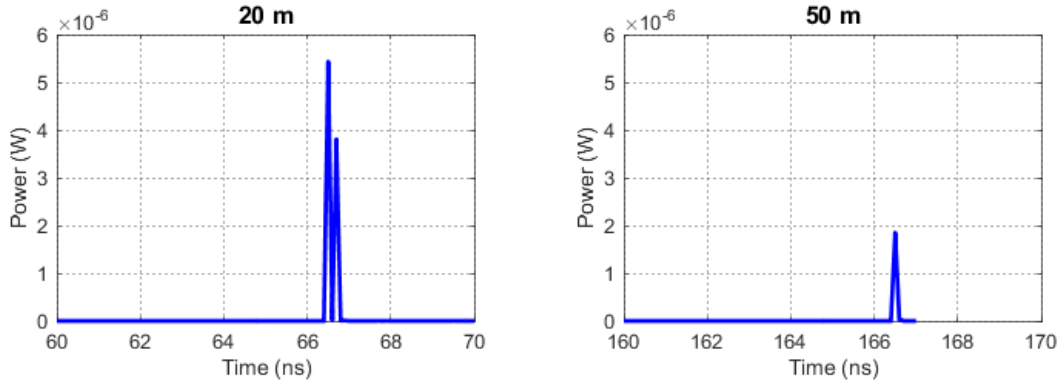

(a)

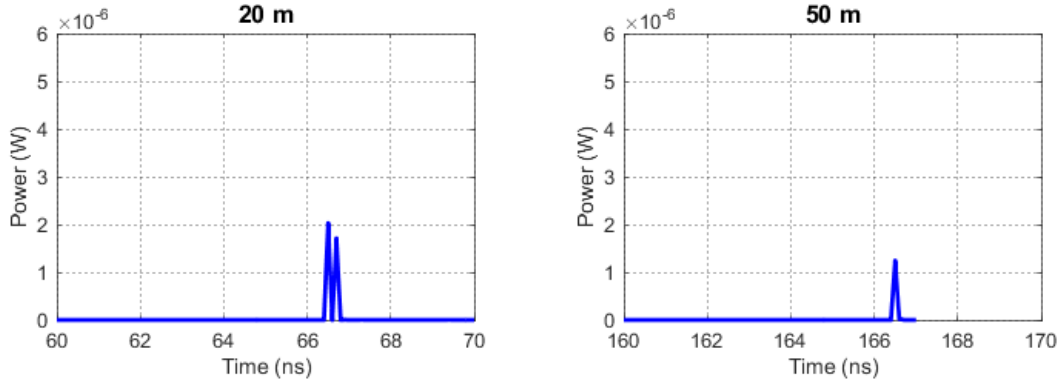

(b)

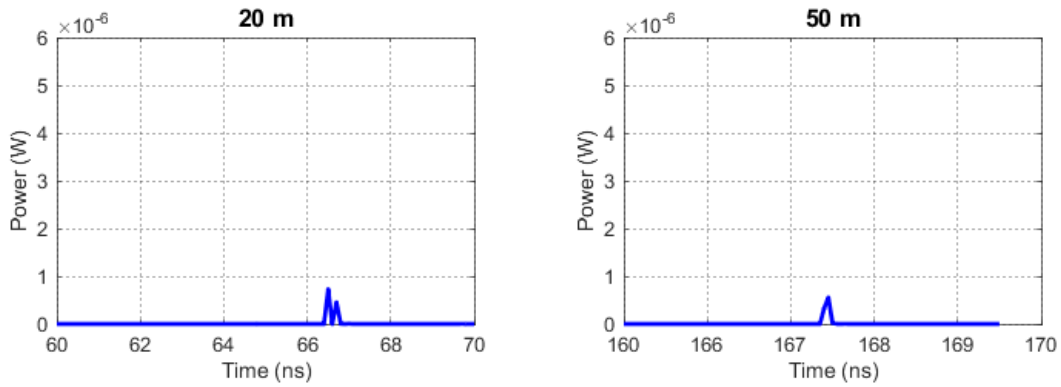

(c)

Fig. 15 Sample CIRs for Scenario IV (a) PD A (b) PD B (c) PD C.

References

[1]. Zemax OpticStudio 18.9. [Online]. Available: https://www.zemax.com/products/opticstudio.

[2]. R. E. Stark, "Road surfaces reflectance influences lighting design", Light. Design Appl., April 1986.

[3]. M. Uysal, C. Capsoni, Z. Ghassemlooy, A. Boucouvalas, and E. Udvary, *Optical wireless communications: an emerging technology*, Springer, 2016.

[4]. M. Elamassie, M. Karbalayghareh, F. Miramirkhani, R. C. Kizilirmak, and M. Uysal, "Effect of fog and rain on the performance of vehicular visible light communications", *IEEE 87th Veh. Technol. Conference (VTC2018-Spring)*, Porto, Portugal, June 2018.

[5]. Specifications of Audi A5 [Online]. Available: https://www.audiusa.com/models/audi-a5-coupe

[6]. P. Colonna, P. Intini, N. Berloco, and V. Ranieri, "Integrated American European protocol for safety interventions on existing two-lane rural roads," *European Transport Research Review*, vol. 10, no. 1, p. 5, 2018.

[7]. UK Department for Transport, *The Installation of Traffic Signals and Associated Equipment*, Sep 1998.

4. Dissemination of results: publications & conferences

- **H. Eldeeb**, F. Miramirkhani, and M. Uysal, "A path loss model for Vehicle-to-Vehicle visible light communications," submitted to 15th International Conference on Telecommunications (ConTEL 2019), Graz, Austria.
- M. Karbalayghareh, F. Miramirkhani, **H. Eldeeb**, K. Refik, S. Sadiq, and M. Uysal, "Performance Characterization of Vehicular Visible Light Communications", under review in *IEEE Transactions on Communications.*